Applied Catalysis A: General xxx (2015) xxx–xxx

Contents lists available at ScienceDirect

Applied Catalysis A: General

journal homepage: www.elsevier.com/locate/apcata

Photocatalytic conversion of CO_2 in water using fluorinated layered double hydroxides as photocatalysts

Shoji Iguchi [a], Kentaro Teramura [a,b,c,*], Saburo Hosokawa [a,b], Tsunehiro Tanaka [a,b,*]

[a] Department of Molecular Engineering, Graduate School of Engineering, Kyoto University, Kyotodaigaku Katsura, Nishikyo-ku, Kyoto 615-8510, Japan
[b] Elements Strategy Initiative for Catalysts & Batteries (ESICB), Kyoto University, 1-30 Goryo-Ohara, Nishikyo-ku, Kyoto 615-8245, Japan
[c] Precursory Research for Embryonic Science and Technology (PRESTO), Japan Science and Technology Agency (JST), 4-1- 8Honcho, Kawaguchi, Saitama 332-0012, Japan

ARTICLE INFO

Article history:
Received 31 August 2015
Received in revised form
10 November 2015
Accepted 13 November 2015
Available online xxx

Keywords:
CO_2 reduction
Photocatalyst
Layered double hydroxide
Fluorination

ABSTRACT

The photocatalytic conversion of CO_2, which can convert CO_2 into useful chemicals, such as CH_4, CH_3OH, HCOOH, HCHO, and CO, is attractive process for creating an artificial carbon cycling system. It was found that the synthetic Ni–Al layered double hydroxide (Ni–Al LDH) can reduce CO_2 into CO in an aqueous solution of NaCl under UV light irradiation, and chloride ions (Cl^-) in the reaction solution scavenge the photogenerated holes. In this study, we prepared fluorinated Mg–Al LDH and Ni–Al LDH for altering the chemical and/or physical properties of the LDH as a solid base, and investigated the effect of fluorination on the photocatalytic activity for the conversion of CO_2 in an aqueous solution. We found that the fluorination of LDH by incorporation of hexafluoroaluminate (AlF_6^{3-}) units in the hydroxide sheets clearly improved the amount of CO evolved as a reduction product of CO_2.

1. Introduction

The development of a chemical process that can fix CO_2 using natural energy sources is necessary for creating an artificial carbon cycling system. The photocatalytic conversion of CO_2 is considered one of the most attractive processes for converting CO_2 into useful chemicals, such as CH_4, CH_3OH, HCOOH, HCHO, and CO, because, in future, it might be able to use solar energy as the driving source. Our research group has previously reported the photocatalytic conversion of CO_2 using H_2 as a reductant over metal oxides such as ZrO_2 [1–4], MgO [5,6], $ATaO_3$ (A = Li, Na, and K) [7], and Ga_2O_3 [8]. The results showed that the adsorbed CO_2 species on the surface of these photocatalysts play an important role in the photocatalytic conversion of CO_2. This indicates that solid base materials that have the ability to provide suitable surface properties for CO_2 adsorption should be promising candidates for this photocatalytic reaction. However, because their basic sites are easily poisoned by water, these metal oxide photocatalysts do not show promising results for the conversion of CO_2 in aqueous solutions. The development of a highly stable photocatalytic system, capable of functioning in water, for the selective conversion of CO_2 is required for the construction of a photocatalytic carbon cycling system.

Layered double hydroxides (LDHs) [9–11], which can function as solid base materials in the presence of water [12], are presented by the general formula $[M^{2+}_{1-z}–M^{3+}_z\ (OH)_2](A^{n-})_{z/n}\cdot mH_2O$. M^{2+} and M^{3+} are the divalent and trivalent cations, respectively. A^{n-} is the interlayer anion of valence n and compensates for the positive charge of the hydroxide sheets. The value z represents the molar ratio of $M^{3+}/(M^{2+}+M^{3+})$ within the hydroxide sheets, and it has been reported that the LDH structure can exist for z values in the 0.1–0.5 range [9]. The nature of M^{2+}, M^{3+}, z, and A^{n-} can be altered over a wide range of values; therefore, by referring to published reports, various isostructural materials with varied chemical properties can be successfully synthesized [13–28]. In recently years, the application of various LDHs to photocatalytic reactions, including the degradation of organic compounds [17,29–33] and water splitting [23,34,35], has been studied. For example, the photocatalytic evolution of H_2 from water using Ni–Ti LDH as the photocatalyst was achieved in the presence of a sacrificial reagent under visible light irradiation [35]. Previously, we applied a series of synthetic LDHs to the photocatalytic conversion of CO_2 in water and found that Ni–Al LDH exhibited high activity for the CO evolution under UV light irradiation [36,37]. The use of Ni–Al LDH enabled the selective formation of CO, because the amount of H_2 evolved by the reduction of H^+ derived from water was much smaller than that of

* Corresponding authors at: Department of Molecular Engineering, Graduate School of Engineering, Kyoto University, Kyotodaigaku Katsura, Nishikyo-ku, Kyoto 615-8510, Japan.
E-mail address: teramura@moleng.kyoto-u.ac.jp (K. Teramura).

http://dx.doi.org/10.1016/j.apcata.2015.11.023
0926-860X/

other LDHs. Moreover, in the presence of Ni–Al LDH, the addition of chloride ion (Cl^-) to the reaction solution enhanced the conversion of CO_2 to CO, and a stoichiometric amount of hypochlorous acid (HClO) was produced by the oxidation of Cl^- [38].

Many attempts have been made to modify the chemical and/or physical properties of LDHs. A series of noble metal particles loaded on the surface of Mg–Al LDH exhibited excellent catalytic activities for dehydrogenation [39], oxidation [40], and reforming [41] processes. The intercalation of different kinds of functional compounds, such as polyoxometalates (POM) [42–44], metal complexes [45,46], and organic dyes [47,48], into the interlayer space of LDHs was presented by many researchers. Moreover, some composite materials with metal oxides, such as TiO_2/Mg–Al LDH [49,50] and CeO_2/Mg–Al LDH [51], have also been reported to improve the photocatalytic activity. In 2012, Lima et al. developed the fluorinated Mg–Al LDH using Na_3AlF_6 as a fluorine source, wherein some $(Al(OH)_6)^{3-}$ octahedral structures within the hydroxide sheets were partially substituted by AlF_6^{3-} units [52]. The fluorination of LDH via intercalation of fluoride anions (F^-) in the interlayer space has also been reported previously [53–55]. It is expected that F^- should ultimately be exchanged with other selective anions such as CO_3^{2-}, because F^- is not stable as a charge compensating anion of LDH. Therefore, the incorporation of fluorine, by substituting the OH groups, as part of the brucite-like hydroxide layer is a new strategy for altering the chemical and/or physical properties of the LDH material as a solid base. In fact, Lima et al. have suggested that, because of its high electronegativity, the incorporation of fluorine as AlF_6^{3-} units into the hydroxide sheets greatly influences the basicity of the LDH [52]. We predict that the CO_2 adsorption on the surface of the LDH is enhanced by the fluorination. Thus, the selectivity toward CO_2 reduction should be improved. In this study, we prepared fluorinated Mg–Al LDH and Ni–Al LDH with different fluorine contents by following the previously reported procedures and investigated the effect of fluorination on the photocatalytic activity for the conversion of CO_2 in an aqueous solution.

2. Experimental

2.1. Catalyst preparation

Fluorinated layered double hydroxides (***F***(***x***) M^{2+}–Al LDH, $M^{2+} = Mg^{2+}$ and Ni^{2+}) were synthesized by a typical coprecipitation method. Precursors of metal components, such as $MgCl_2{\cdot}6H_2O$ or $NiCl_2{\cdot}6H_2O$, $AlCl_3$, and Na_3AlF_6, were dissolved in 1.0 L of ultrapure water. The value of ***x*** in ***F***(***x***) M^{2+}–Al LDH means a ratio of Na_3AlF_6 in the total Al species ($AlCl_3 + Na_3AlF_6$) when preparing it. The aqueous solution of precursors was dropped into an aqueous solution of Na_2CO_3 at room temperature with vigorous stirring. The pH of the suspension was strictly kept between 9.9 to 10.1 by using a pH controller (NPH-660NDE, Nissin Rika) equipped with a liquid feeding pump for an aqueous solution of NaOH. The resulting suspension was aged at 333 K for 12 h, and then collected by filtration. The solid precipitate was washed with 1.0 L of ultra-pure water and dried at 383 K in air atmosphere. The atomic ratio of M^{2+} to Al^{3+} (M^{2+}/Al^{3+}, $M^{2+} = Mg^{2+}$ and Ni^{2+}) was fixed at 3 in all samples. ***F***(7.5) imp- Ni–Al LDH was prepared as a reference sample via an impregnation method. ***F***(0) Ni–Al LDH powder was dispersed in an aqueous solution which contains a required amount of Na_3AlF_6, and the suspension was dried up at 353 K under air atmosphere.

2.2. Catalyst characterization

The powder XRD patterns of a series of prepared LDHs were measured by an X-ray diffractometer (MultiFlex, Rigaku) using Cu $K\alpha_1$ radiation ($\lambda = 0.154$ nm) at a scan rate of 4.0° min^{-1}. UV/vis diffuse reflection spectra of LDHs were collected on a UV–visible Spectrometer (V-650, JASCO) equipped with an integrated sphere accessory. Thermal analysis for the synthesized LDHs were carried out using a thermobalance (Thermo Plus 2, Rigaku) under dried air atmosphere at a flow rate of 80 mL min^{-1}. The specific surface areas of samples were estimated from the N_2 adsorption isotherms at 77 K using a surface area analyzer (BELSORP-miniII, BEL Japan, Inc.). Prior to the measurements, LDHs were evacuated at 383 K for 1 h using a pretreatment instrument (BELPREP-vacII, BEL Japan, Inc.). X-ray photoelectron spectra (XPS) profiles of the synthesized LDHs were collected by an X-ray photoelectron spectrometer (ESCA 3400, Shimadzu Corp.). The narrow range scans for Ni 2p and F 1s spectra were performed using an Mg Kα X-ray source, and the peak positions were calibrated by the peak that can be attributed to C 1s. The peak intensity of F 1s spectra was normalized with that of Ni $2p_{3/2}$ peak.

2.3. Photocatalytic conversion of CO_2 in an aqueous solution

The photocatalytic activity of synthesized ***F***(***x***) M^{2+}–Al LDHs ($M^{2+} = Mg^{2+}$ or Ni^{2+}) for the conversion of CO_2 in water were evaluated by using a quartz inner-irradiation type reaction vessel connected to the closed circulation system. 0.5 g of photocatalyst powder was dispersed in 350 mL of ultra-pure water, and the suspension was degassed at room temperature. 7.6 mmol of CO_2 gas, which was purified by a vacuum distillation at liquid N_2 temperature, was introduced into the free gas space. The suspension was irradiated under a 400 W high-pressure Hg lamp (HL400BH-9, SEN LIGHTS Corp.) through a quartz filter equipped with a cooling water system. The gas phase products were analyzed by a thermal conductivity detector gas chromatography (TCD-GC) using a GC-8A chromatograph (GC-8AIT, Shimadzu Corp.) fitted out a MS-5A packed column. GC–MS analysis was performed using a quadruple-type mass spectrometer (BEL Mass, BEL Japan, Inc.) in the case of an isotopic experiment. The selectivity toward CO evolution among reduction products was calculated by following equation.

Selectivity toward CO evolution (%) $= 100 \times A_{CO}/(A_{CO} + A_{H2})$

A_{CO}: amount of CO evolved / μmol

A_{H2}: amount of H_2 evolved / μmol

The amount of HClO produced in the reaction solutions was determined by a DPD (*N*,*N*′-dimethyl-*p*-phenylenediamine) method [56,57], which is one of the most popular techniques to observe HClO in water. The DPD solution was prepared by dissolving 0.06 g of the DPD reagent, which is a mixture of DPD sulphate and Na_2SO_4, in 3.0 mL of phosphate buffer solution (pH 6.5). Following this, 1.0 mL of the prepared DPD solution was added to 5.0 mL of the sample solution, and was shaken for 20 s. The transmittance spectrum was measured immediately using a multiscan UV–vis spectrometer (MCPD-7700, Otsuka Electronics Co., Ltd.). The concentration of HClO in the aqueous solution was estimated from the absorbance at 515 nm.

3. Results and discussion

Fig. 1 displays the XRD patterns of ***F***(0) Mg–Al LDH and ***F***(5) Mg–Al LDH collected over (a) a wide and (b) a narrow range of angles, respectively. Both diffraction patterns corresponded with the typical structure of the LDH group; i.e., the layered structure of the hydroxide sheets grew along the *c*-axis with respect to the hexagonal crystalline units. As reported by Lima et al. [52], three sharp reflection peaks observed at around 11.4°, 22.9°, and 34.6° in the XRD pattern of the fluorinated Mg–Al LDH were assigned to the (0 0 3), (0 0 6), and (0 0 9) phases, respectively. These reflections are related to the thickness of the layer structure, especially the d-spacing of the (0 0 3) phase ($d_{(003)}$), which corresponds to

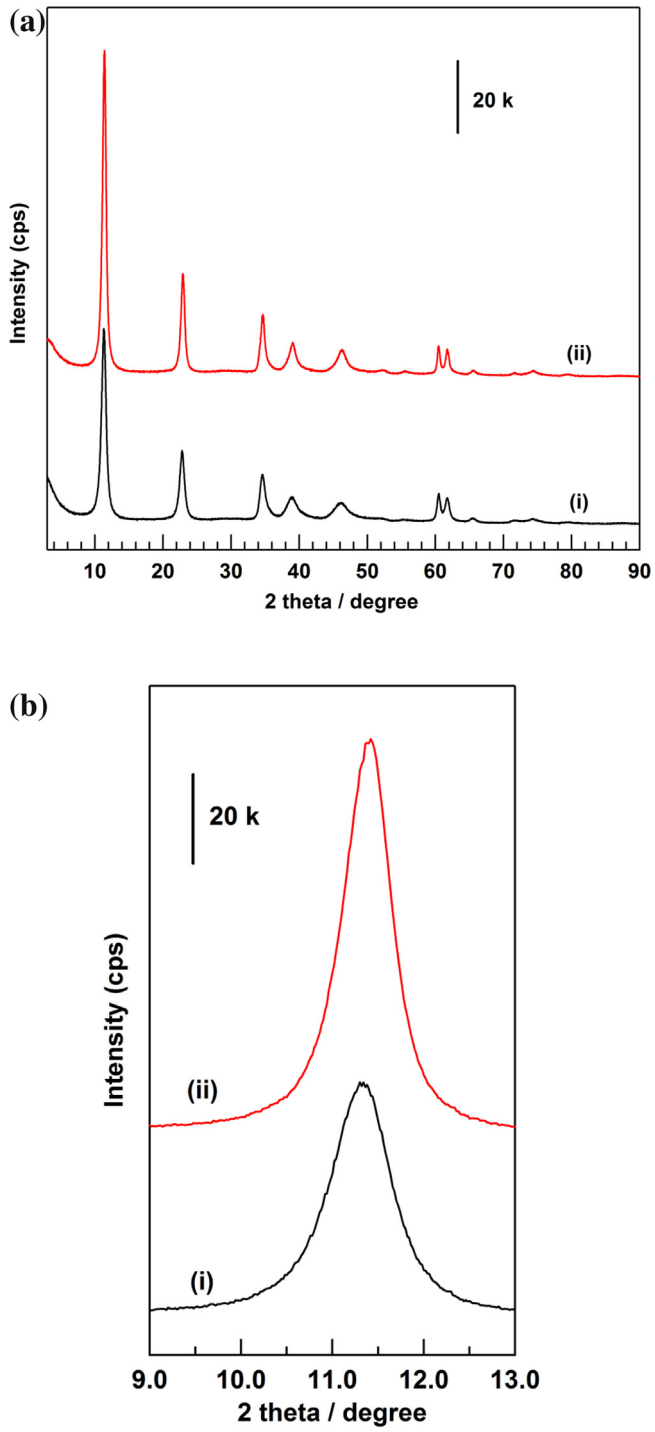

Fig. 1. XRD patterns of (i) ***F***(0) Mg–Al LDH (black) and (ii) ***F***(5) Mg–Al LDH (red) collected over (a) a wide and (b) a narrow range of angles. (For interpretation of the references to color in this figure legend, the reader is referred to the web version of this article.)

the interval of adjacent hydroxide sheets. It is well known that the intercalation of anions, which have large ionic radii, results in an increase in the layer distance in the LDH structure. For example, the peak position of the (0 0 3) phase was shifted to a lower angle by the incorporation of organic dye anions or metal oxy anions. Carriazo et al. reported that Mg–Al LDH, which contains $(H_2W_{12}O_{40})^{6-}$ as an interlayer charge compensating anion, shows (0 0 3) phase diffraction peak at around 6.1° (2θ, Cu Kα_1) [43]. Taking this into account, the presence of AlF_6^{3-} anion in the interlayer space of LDH should shift the peak of the (0 0 3) phase reflection to a lower angle because of the bulky structure of AlF_6^{3-}; in contrast, the ionic radius of CO_3^{2-} is 178 pm [58]. The fluorination of LDH via the incorporation of the AlF_6^{3-} unit into hydroxide sheets did not change the interlayer distance, which indicated that AlF_6^{3-} units were not present in the interlayer space. On the other hand, the peak position of the (0 0 3) phase diffraction peak was shifted slightly to a higher angle, as shown in Fig. 1(b) . This change indicated that the decrease in interlayer distance was caused by fluorination. Lima et al. proposed that the enhancement of hydrogen-bonding between the hydroxide sheets and interlayer water molecules decreased the interval between hydroxide sheets, because fluorine is one of the most electronegative elements [52]. Other intense peaks located above 60° are attributed to the (1 1 0) and (1 1 3) phase reflections. The cation-to-cation distance within the hydroxide sheet (parameter a) can be calculated using the d-spacing of the (1 1 0) phase reflection ($a = 2d_{(1\,1\,0)}$). The peak position of the (1 1 0) phase diffraction was not influenced by the fluorination of hydroxide sheets, indicating that parameter a remained unchanged. Lima et al. presented the MAS NMR results of ^{27}Al and ^{19}F and reported that the AlF_6^{3-} units should be incorporated randomly in the hydroxide sheets [52]. Weight loss curves of ***F***(0) Mg–Al LDH and ***F***(5) Mg–Al LDH, obtained using thermal gravimetric analysis are presented in Fig. 2(a). The LDH group structure shows weight loss in two steps. The first weight loss happens below 473 K and is attributed to the desorption of water molecules from the interlayer. The second loss takes place between 473 and 673 K and is attributed to two phenomena, viz. the decomposition of interlayer charge-compensating anions and the dehydration of hydroxide sheets accompanied by the collapse of the layer structure. Both ***F***(0) and ***F***(5) Mg–Al LDHs exhibited similar weight loss curves. No changes were observed with regards to the weight loss temperature and the extent of weight loss. These results indicated that the fluorination of Mg–Al LDH influenced neither the stability of hydroxide sheets nor the amount of carbonate ions preserved in the interlayer space. Fig. 2(b) shows the UV/vis diffuse reflectance spectra of ***F***(0) and ***F***(5) Mg–Al LDHs. Both the shape of the spectrum and the absorption edge were not changed by the fluorination of Mg–Al LDH. On the other hand, Na_3AlF_6 powder exhibited no absorption peak in the 200–800 nm range. The fluorination of Mg–Al LDH via incorporation of AlF_6^{3-} units into the hydroxide sheets did not change the absorption spectrum. In the present study, the fluorination of LDH is not considered "doping", but is considered a "solid solution". This is because fluorine atoms are present as a component of the AlF_6^{3-} units in the brucite-like hydroxide sheets.

Fig. 3(a) displays the time courses of CO evolution in the photocatalytic conversion of CO_2 in an aqueous NaCl solution using ***F***(5) Mg–Al LDH photocatalyst. ***F***(5) Mg–Al LDH photocatalyst could reduce CO_2 under UV light irradiation, and CO and H_2 were evolved with high stability as the reduction product of CO_2 and proton (H^+), respectively. Other reduction products, such as methane, methanol, formaldehyde, and formic acid were not produced in this photocatalytic reaction system. We previously reported that the addition of Cl^- in the reaction solution improves the activity for the photocatalytic conversion of CO_2 into CO over Ni–Al LDH because Cl^- acts as a hole scavenger [38] and hence advances the conversion. It is proposed that Cl^- in the reaction solution enhances CO formation based on the same mechanism as in the case of Ni–Al LDH; i.e., Cl^- captures the photogenerated holes and it should be oxidized to Cl_2. As shown in Fig. 3(b), the photocatalytic activity for CO formation over ***F***(0) Mg–Al LDH was also enhanced by the addition of Cl^-. Moreover, the fluorination of Mg–Al LDH obviously increases the amount of CO evolved in the photocatalytic conversion of CO_2 in an aqueous NaCl solution (see difference between (ii) and (iv)). In this case, the amount of CO produced for ***F***(5) Mg–Al LDH was twice that for ***F***(0) Mg–Al LDH. On the other hand, the amount of H_2

Please cite this article in press as: S. Iguchi, et al., Appl. Catal. A: Gen. (2015), http://dx.doi.org/10.1016/j.apcata.2015.11.023

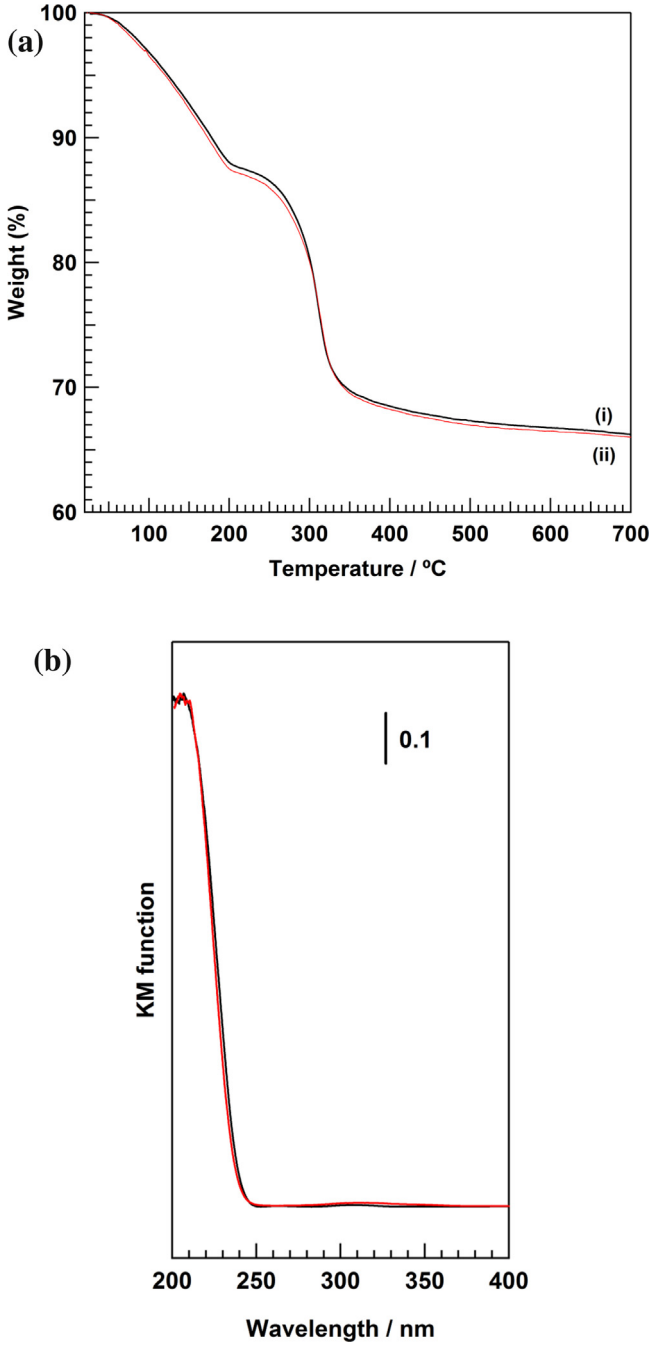

Fig. 2. (a) Weight loss curves in thermal gravimetric analysis and (b) UV/vis diffuse reflectance spectra of (i) ***F***(0) Mg–Al LDH (black) and (ii) ***F***(5) Mg–Al LDH (red). (For interpretation of the references to color in this figure legend, the reader is referred to the web version of this article.)

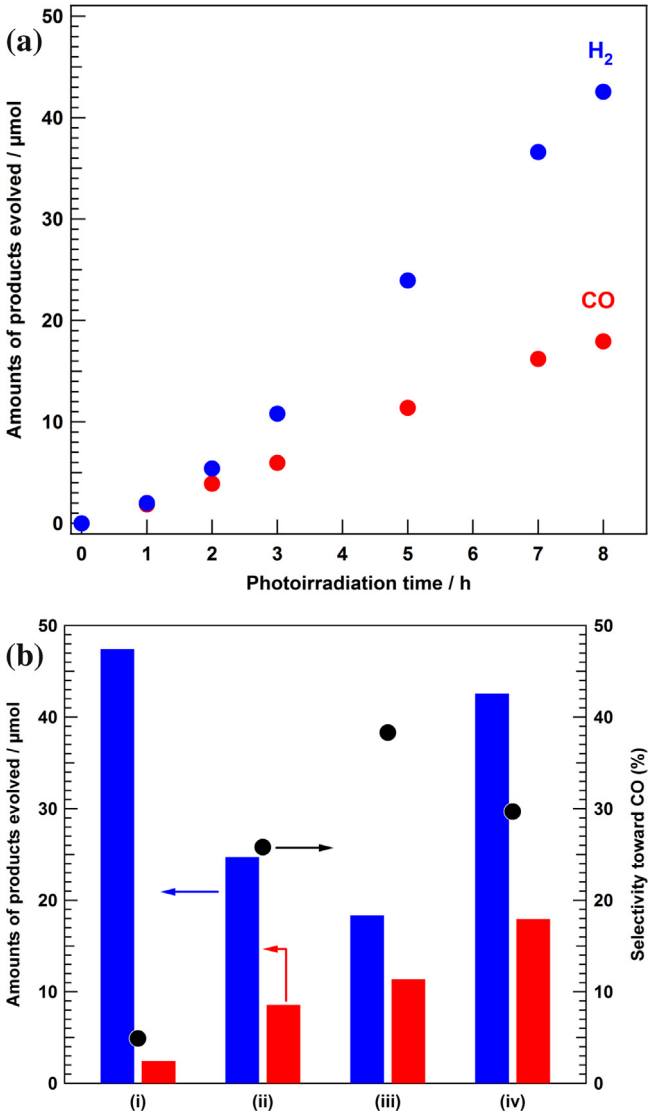

Fig. 3. (a) Time courses of H_2 (blue) and CO (red) evolution in the photocatalytic conversion of CO_2 in an aqueous NaCl solution (0.1 M) using ***F***(5) Mg–Al LDH photocatalyst. (b) Total amounts of H_2 (blue) and CO (red) after 8 h of photoirradiation in the photocatalytic conversion of CO_2 in water. (i) ***F***(0) Mg–Al LDH photocatalyst with no additive, (ii) ***F***(0) Mg–Al LDH photocatalyst with 0.1 M of NaCl additive, (iii) ***F***(5) Mg–Al LDH photocatalyst with no additive, and (iv) ***F***(5) Mg–Al LDH photocatalyst with 0.1 M of NaCl additive. The selectivity toward CO among reduction products is presented with black circle in Fig. 3(B). Photocatalyst weight: 500 mg, water: 350 mL, CO_2: 7.6 mmol, light source: 400 W high-pressure Hg lamp (quartz jacket). (For interpretation of the references to color in this figure legend, the reader is referred to the web version of this article.)

evolved was also affected by both Cl^- addition and the fluorination of Mg–Al LDH (by comparing (i) and (ii) in Fig. 3(b)). It is well known that selective CO_2 reduction is one of the most important indices of photocatalytic activity for CO_2 conversion in water, because the reduction of protons (H^+) takes place competitively in this reaction. In this regard, ***F***(5) Mg–Al LDH enabled the improvement in selectivity toward CO formation in an aqueous NaCl solution. Hence, we propose that the fluorination of Mg–Al LDH leads to an enhancement in both the amount of CO evolved and the selectivity toward CO formation.

As described in our previous work, the amount of CO evolved for Ni–Al LDH is larger than that for Mg–Al LDH, and the use of Ni–Al LDH as a photocatalyst particularly suppresses H_2 formation. Therefore, Ni–Al LDH is considered one of the most favorable photocatalysts for selective CO_2 in an aqueous solution [37]. Fig. 4(a) shows the XRD patterns of ***F***(***x***) Ni–Al LDH (***x*** = 0, 2.5, 5, 7.5, 10 and 20) and Na_3AlF_6, which was used as a precursor for the AlF_6^{3-} unit. The typical diffraction patterns corresponding to the LDH structure were observed over the entire range of ***x*** values without any impurity phases such as $Ni(OH)_2$, $Al(OH)_3$, NaF, and Na_3AlF_6. This indicated that the fluorinated Ni–Al LDHs were successfully synthesized via the co-precipitation method. Fig. 4(b–d) show the XRD patterns of ***F***(***x***) Ni–Al LDH (***x*** = 0, 2.5, 5, 7.5, 10 and 20) collected in a narrow range to observe details of the (0 0 3), (0 0 6), and (1 1 0) phase reflections, respectively. As discussed above, the intercalation of AlF_6^{3-} in the interlayer of the hydroxide sheets should cause an increase in the interlayer distance ($d_{(003)}$). However, the (0 0 3)

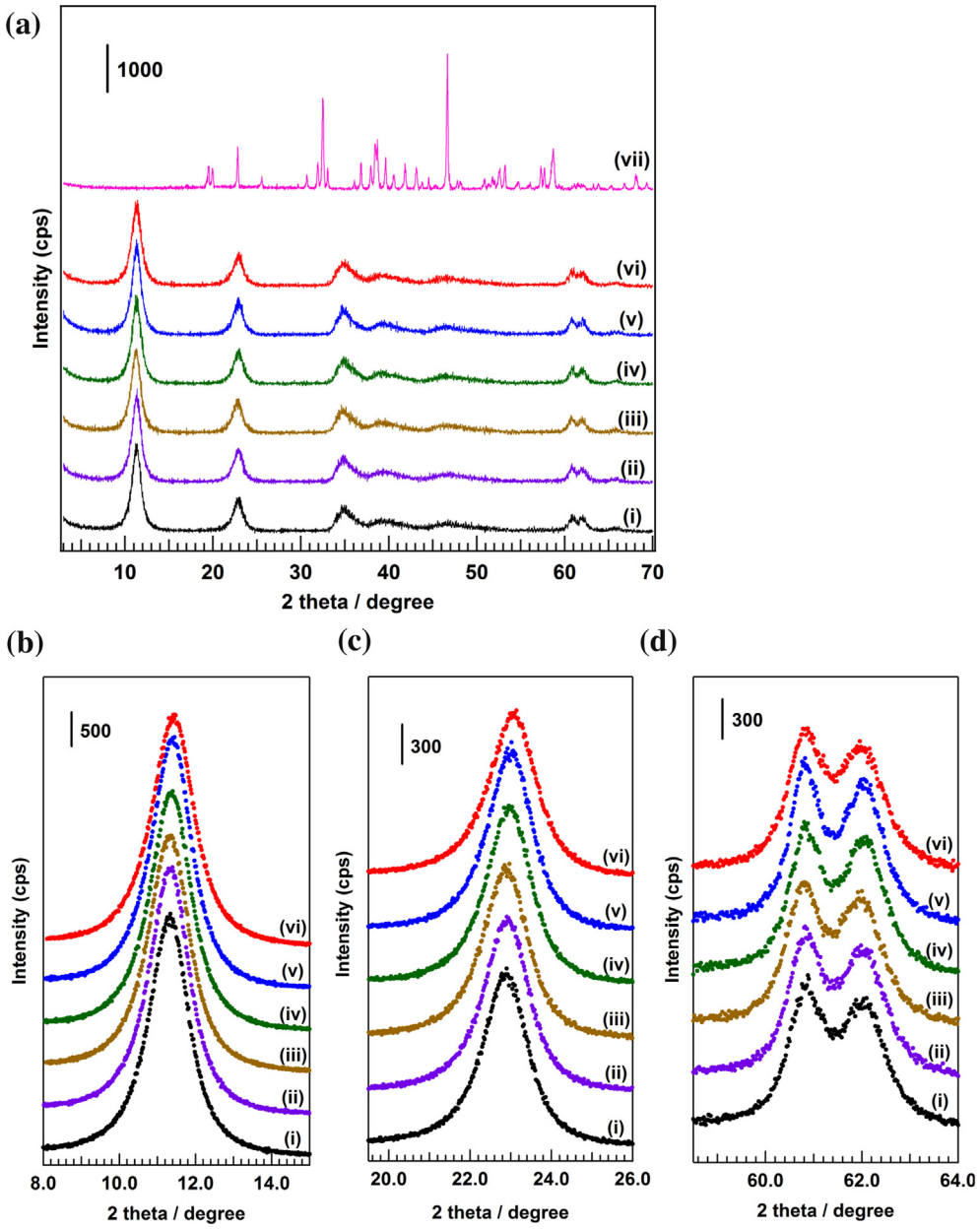

Fig. 4. XRD patterns of ***F*(*x*)** Ni–Al LDH and Na_3AlF_6 collected over (a) a wide range and a narrow ranges of angles for (b) (0 0 3) phase, (c) (0 0 6) phase, and (d) (1 1 0) phase reflections. ***x*** = (i) 0, (ii) 2.5, (iii) 5.0, (iv) 7.5, (v) 10, (vi) 20, and (vii) Na_3AlF_6.

Table 1
Peak positions of (0 0 6) and (1 1 0) phase reflections in the XRD patterns, the calculated value of $d_{(003)}$, the specific surface area (S_{BET}), and the result of the photocatalytic activity test for ***F*(*x*)** Ni–Al LDH (***x*** = 0, 2.5, 5, 7.5, 10, and 20). Photocatalyst weight: 500 mg, water: 350 mL, CO_2: 7.6 mmol, light source: 400 W high-pressure Hg lamp (quartz jacket), photoirradiation time: 8 h.

χ	Position / degree		$d_{(003)}$ / Å	S_{BET} / m^2g^{-1}	Amounts of products / μmol		Selectivity (%)
	(0 0 6)	(1 1 0)			CO	H_2	
0	22.90	60.88	7.76	75.1	18.8	20.6	47
2.5	22.92	60.82	7.75	83.4	30.0	8.0	79
5.0	22.95	60.80	7.75	113	36.8	7.0	84
7.5	22.97	60.80	7.74	113	47.3	12.0	80
10	23.00	60.82	7.73	120	31.7	14.1	69
20	23.10	60.82	7.70	86.3	18.5	12.6	59

and (0 0 6) phase diffraction peaks of Ni–Al LDH, which are related to the thickness of the layer structures, shifted to slightly higher angles with an increase in the fluorination rate. This result indicated that the marginal decrease in layer distance was caused by the incorporation of fluorine species in the hydroxide sheets of Ni–Al LDH, which was consistent with the results obtained by Lima et al. [52]. Table 1 lists the position of the (0 0 6) and (1 1 0) phase reflections in the XRD patterns, the calculated value of $d_{(003)}$, the specific

surface area (S_{BET}), and the results of the photocatalytic activity test for ***F***(***x***) Ni–Al LDH (***x*** = 0, 2.5, 5, 7.5, 10, and 20). The distance between adjacent hydroxide sheets ($d_{(003)}$), which was calculated from the position of the (0 0 6) phase reflection in this study, gradually decreased with an increase in the amount of AlF_6^{3-} units in the hydroxide sheets. However, the position of the (1 1 0) phase diffraction peak was not influenced by fluorination. The amount of CO evolved after 8 h of photoirradiation was affected by the fluorination of Ni–Al LDH, and ***F***(7.5) Ni–Al LDH exhibited the highest activity for CO formation. In particular, 47.3 μmol of CO was produced after 8 h of photoirradiation using ***F***(7.5) Ni–Al LDH in the photocatalytic conversion of CO_2 in an aqueous NaCl solution. It was found that the excess AlF_6^{3-} incorporation (***x*** = 10 and 20) caused a decrease in the photocatalytic conversion of CO_2 to CO. On the other hand, ***F***(2.5) Ni–Al LDH produced less H_2 than ***F***(0) Ni–Al LDH, indicating that fluorination altered the selectivity toward CO formation among the reduction products. In fact, after 8 h of photoirradiation, the selectivity toward CO clearly changed with the extent of fluorination (as shown in Table 1). By comparing with the results previously reported from our group [37], the photocatalytic activity of Ni–Al LDH was clearly improved by the tuning of the reaction condition (addition of NaCl) and the chemical properties of photocatalyst itself (fluorination). Furthermore, the actual amount of CO_2 reduction product, 47.3 μmol of CO after 8 h of photoirradiation in this study, is much larger value than others reports using LDHs photocatalysts for the conversion of CO_2 [59–62]. As presented in Table 1, the specific surface area of ***F***(***x***) Ni–Al LDH was also influenced by the value of ***x***. For ***x*** = 5, 7.5, and 10, the results showed relatively larger surface areas. We have already reported that the amount of CO evolved in the photocatalytic conversion of CO_2 in an aqueous NaCl solution using Ni–Al LDH strongly depends on the surface area. This means that Ni–Al LDH with a large specific surface area can achieve higher photocatalytic activity for the conversion of CO_2 to CO because the adsorption of CO_2 molecules on the surface of photocatalyst materials is an innegligible step to convert CO_2 [38]. Therefore, an increase in the specific surface area is one of the reasons for the enhanced formation of CO upon fluorination of Ni–Al LDH. Meanwhile, another change in the physical and/or chemical properties because of fluorination would cause the difference in selectivity toward CO formation. Lima et al. suggested that fluorine incorporation into LDH hydroxide sheets leads to the formation of strong basic sites [52]. We presume that the change in surface properties has a critical influence on the adsorption features of CO_2 molecules and the selectivity toward CO formation is therefore improved via suppression of H_2 evolution by the fluorination of Ni–Al LDH. In other words, the fluorination of the hydroxide sheets would impart surface properties that facilitate the conversion of CO_2 to CO in aqueous solution. This is because the adsorbed CO_2 species on the surface of LDH are considered responsible for this reaction. More detailed information, such as changes in the amount of adsorbed CO_2, the heat of adsorption for CO_2 upon fluorination and the adsorbed CO_2 species under the reaction conditions, is now being obtained in further investigations.

Fig. 5 presents the results of various blank tests for the photocatalytic conversion of CO_2 in an aqueous solution using ***F***(7.5) Ni–Al LDH as the photocatalyst. No photocatalytic activity was observed without photoirradiation (see Fig. 5(F)). Table 1 shows that the fluorination of Ni–Al LDH (***x*** = 7.5) clearly improved CO formation, while simultaneously suppressing the H_2 evolution (see Figs. 5(A) and (B)). The addition of Na_3AlF_6, which was used as a precursor to AlF_6^{3-} units, did not improve the activity for CO formation over ***F***(0) Ni–Al LDH (see Fig. (C)). The use of ***F***(7.5) imp- Ni–Al LDH, which is prepared via an impregnation method and wherein all AlF_6^{3-} units are present on the surface of ***F***(0) Ni–Al LDH, did not result in the enhancement of CO evolution. These results indicated that the incorporation of AlF_6^{3-} units in the hydroxide sheets significantly

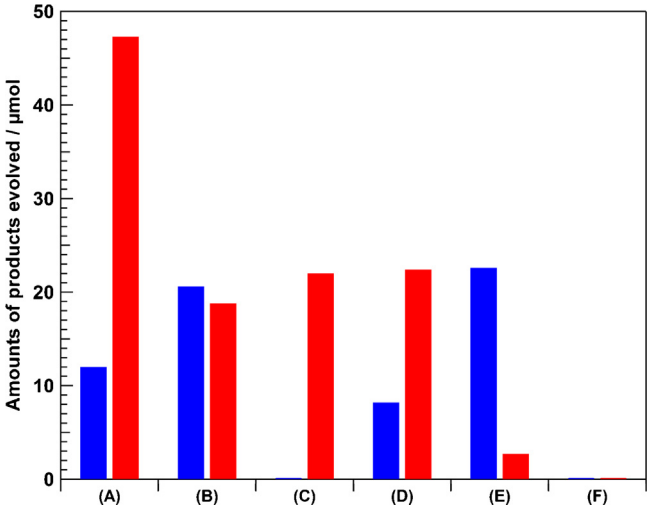

Fig. 5. Total amounts of H_2 (blue) and CO (red) after 8 h of photoirradiation in the photocatalytic conversion of CO_2 in an aqueous solution of NaCl. (A) ***F***(7.5) Ni–Al LDH, (B) ***F***(0) Ni–Al LDH, (C) ***F***(0) Ni–Al LDH (Na_3AlF_6 was dissolved into the reaction solution as a second additive), (D) ***F***(7.5) imp-Ni–Al LDH, (E) ***F***(7.5) Ni–Al LDH without CO_2 (Ar was introduced instead of CO_2), and (F) ***F***(7.5) Ni–Al LDH without irradiation. Photocatalyst weight: 500 mg, water: 350 mL, additive: NaCl 0.1 M, CO_2: 7.6 mmol (except for (E)), light source: 400 W high-pressure Hg lamp (quartz jacket), photoirradiation time: 8 h. (For interpretation of the references to color in this figure legend, the reader is referred to the web version of this article.)

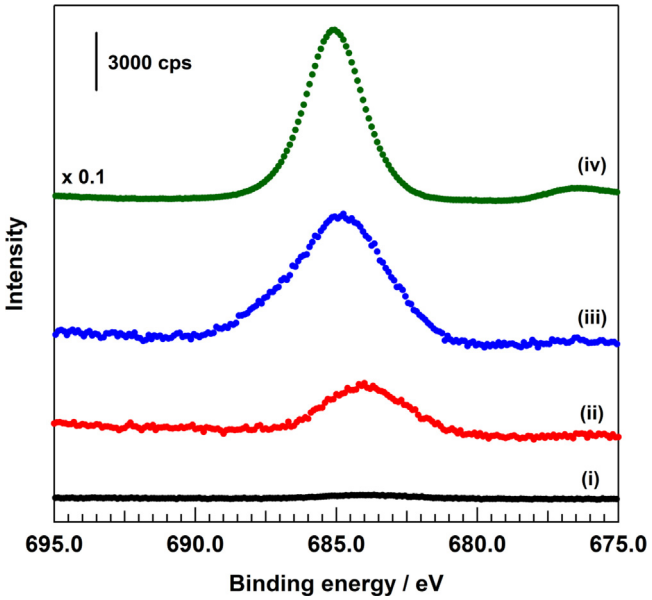

Fig. 6. F 1s XPS profiles of (i) ***F***(0) Ni–Al LDH, (ii) ***F***(7.5) Ni–Al LDH, (iii) ***F***(7.5) imp-Ni–Al LDH, and (iv) Na_3AlF_6. The intensities of (i), (ii), and (iii) were normalized with that of Ni $2p_{3/2}$ peak.

improved the photocatalytic conversion of CO_2 to CO. To confirm the existence of AlF_6^{3-} units on the surface of ***F***(7.5) Ni–Al LDH and ***F***(7.5) imp- Ni–Al LDH, F 1s X-ray photoelectron spectroscopy was performed (as shown in Fig. 6**)** . The peak at around 684.0 eV in the profile of ***F***(7.5) Ni–Al LDH suggested that fluorine atoms were present on the surface of this material. However, no peak was observed in the profile of ***F***(0) Ni–Al LDH. Furthermore, the normalized intensity of ***F***(7.5) imp- Ni–Al LDH was larger than that of ***F***(7.5) Ni–Al LDH, indicating that the concentration of AlF_6^{3-} units on the surface was higher in ***F***(7.5) imp- Ni–Al LDH than it was in ***F***(7.5) Ni–Al LDH. The peak position of ***F***(7.5) Ni–Al LDH shifted to a slightly lower binding energy in comparison to that of ***F***(7.5) imp- Ni–Al

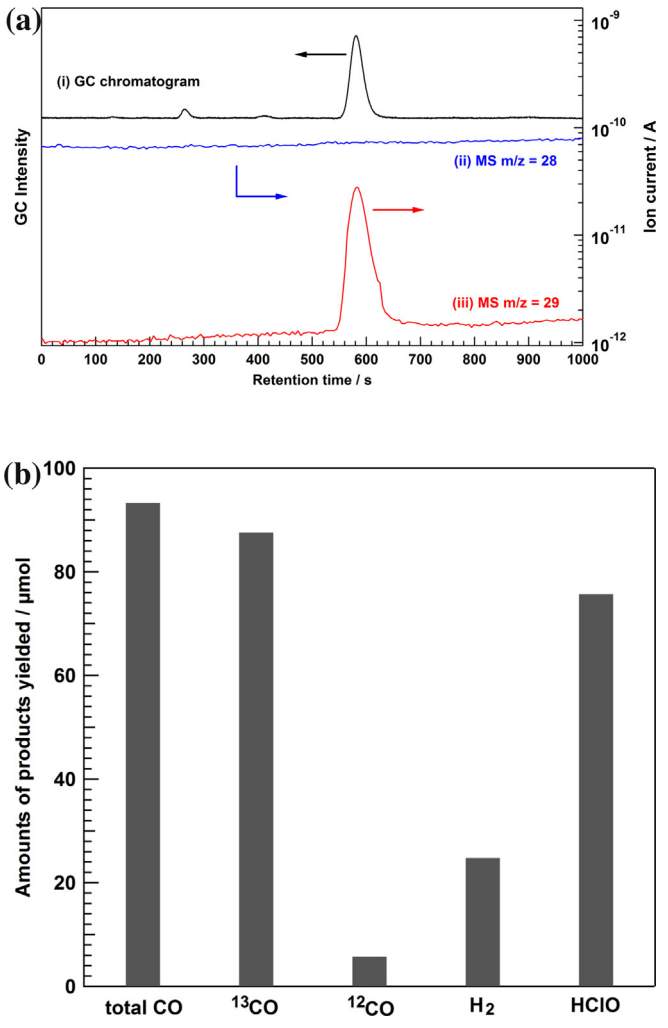

Fig. 7. (a) GC–MS chromatogram for the photocatalytic conversion of ^{13}C-labeled CO_2 in an aqueous solution of NaCl using ***F***(7.5) Ni–Al LDH as a photocatalyst. (i) GC chromatogram detected by TCD, ion current profile of (ii) $m/z = 28$, and (iii) $m/z = 29$. (b) Amounts of products yielded after 20 h of photoirradiation quantified by using the TCD-GC for "total CO" and "H_2", the Q-Mass for "^{13}CO", and the DPD test for "HClO".

LDH, while the peak of ***F***(7.5) imp- Ni–Al LDH was found at almost the same position as Na_3AlF_6. This result provides strong evidence in support of the hypothesis stating that AlF_6^{3-} units are randomly incorporated in the hydroxide sheets, because the fluorine atoms of the AlF_6^{3-} units that constitute the hydroxide sheets are negatively charged. In other words, fluorine atoms that participate in the structure of Ni^{2+}–F–Al^{3+} within the hydroxide sheets have a higher negative charge than those in bare AlF_6^{3-} units (Al^{3+}–F–Al^{3+}). The F 1s XPS profile results reflect this change in the environment of fluorine atoms along with the incorporation of AlF_6^{3-} units in the $Ni(OH)_2$ structure.

Fig. 5(E) shows that a certain amount of H_2 and a small amount of CO were produced when, instead of CO_2, Ar was introduced. The CO evolved in this experiment originated from the naturally adsorbed CO_2 species and/or the CO_3^{2-} preserved in the interlayer space. Fig. 7(a) shows the results of GC–MS analysis for the photocatalytic conversion of ^{13}C-labeled CO_2 (99 atom% of the isotopic purity) in an aqueous NaCl solution using ***F***(7.5) Ni–Al LDH as the photocatalyst. GC–MS analysis was conducted to reveal the carbon source of the product. The peak at 600 s in GC chromatogram is assigned to CO. The sharp peak in the profile of $m/z = 29$, which can be found at the same retention time, is attributed to ^{13}C-labeled CO. This indicated that the carbon source of CO evolved in this photocatalytic system is the CO_2 gas that was introduced as a substrate. In addition, Fig. 7(b) displays the amounts of products produced after 20 h of photoirradiation for the photocatalytic conversion of ^{13}C-labeled CO_2 using ***F***(7.5) Ni–Al LDH. The total amount of CO evolved ($^{12}CO + {}^{13}CO$), which was evaluated by TCD-GC, was 93.3 μmol, whereas the amount of H_2 evolved was 24.7 μmol. These results indicated that the selectivity toward CO among the reduction products was around 80% after 20 h of photoirradiation. By determination of peak area in the profile of $m/z = 29$, it was estimated that almost 94% of the CO evolved was ^{13}C-labled CO. Since it is difficult to detect small amount of unlabeled CO because of the high base level of the $m/z = 28$ peak, which is attributed to the contaminated air in the Q-Mass apparatus, the quantification of ^{13}CO using the profile of $m/z = 29$ is necessary for confirming the actual origin of CO. Additionally, a certain amount of HClO was produced as an oxidation product in the reaction solution. As previously reported by our group, HClO is formed via disproportionation of Cl_2 in water, which is formed by the oxidation of Cl^- [38]. We previously confirmed the stoichiometric formation of HClO via two-electron oxidation of Cl^-, which can be detected by the DPD test [56,57], with the evolution of reduction products such as CO and H_2 over Ni–Al LDH. In the present study, the amount of HClO produced in the reaction solution was less than the stoichiometric amount, which indicated that some of the photogenerated holes have been scavenged by another process. The photocatalytic activity clearly decreased in the absence of NaCl additive. Therefore, we conclude that the photocatalytic conversion of CO_2 to CO over fluorinated Ni–Al LDH (***F***(***x***) Ni–Al LDH) in an aqueous NaCl solution proceeds using Cl^- as a hole scavenger. The results also show that the fluorination of LDH by incorporation of AlF_6^{3-} units in hydroxide sheets affords surface properties suitable for the photocatalytic conversion of CO_2 in the presence of Cl^-. Moreover, the structural change was not observed in ***F***(7.5) Ni–Al LDH which was used in the photocatalytic conversion of CO_2 for 20 h as compared to that before the reaction, indicating that the stability of the fluorinated Ni–Al LDH photocatalyst is considered to be sufficient for the use in the photocatalytic reactions.

4. Conclusion

We found that the fluorination of Mg–Al LDH and Ni–Al LDH improved the photocatalytic conversion of CO_2 to CO in an aqueous NaCl solution under UV light irradiation. After 20 h of photoirradiation over ***F***(7.5) Ni–Al LDH, the amount of CO evolved via reduction of CO_2 and the selectivity toward CO among the reduction products were 93.3 μmol and 80%, respectively. When compared to ***F***(7.5) imp- Ni–Al LDH, the incorporation of AlF_6^{3-} units in the hydroxide sheets causes significant improvement in the photocatalytic conversion of CO_2 to CO. The isotopic experiment revealed that almost all of the evolved CO originated from the CO_2 gas that was introduced as a substrate. In addition, a certain amount of hypochlorous acid (HClO) was produced as an oxidation product in the reaction solution. We conclude that the fluorination of LDH by incorporation of AlF_6^{3-} units in the hydroxide sheets affords surface properties suitable for the photocatalytic conversion of CO_2 in the presence of Cl^-, which acts as a hole scavenger.

Acknowledgments

This study was partially supported by a Grant-in-Aid for Scientific Research on Innovative Areas "All Nippon Artificial Photosynthesis Project for Living Earth" (No. 2406) of the Ministry of Education, Culture, Sports, Science, and Technology (MEXT) of Japan, the Precursory Research for Embryonic Science and Tech-

nology (PRESTO), supported by the Japan Science and Technology Agency (JST), and the Program for Element Strategy Initiative for Catalysts & Batteries (ESICB), commissioned by the MEXT of Japan. Shoji Iguchi thanks the JSPS Research Fellowships for Young Scientists.

References

[1] Y. Kohno, T. Tanaka, T. Funabiki, S. Yoshida, Chem. Commun. (1997) 841–842.
[2] Y. Kohno, T. tanaka, T. Funabiki, S. Yoshida, Chem. Lett. 26 (1997) 993–994.
[3] Y. Kohno, T. Tanaka, T. Funabiki, S. Yoshida, J. Chem. Soc. Faraday Trans. 94 (1998) 1875–1880.
[4] Y. Kohno, T. Tanaka, T. Funabiki, S. Yoshida, Phys. Chem. Chem. Phys. 2 (2000) 2635–2639.
[5] Y. Kohno, H. Ishikawa, T. Tanaka, T. Funabiki, S. Yoshida, Phys. Chem. Chem. Phys. 3 (2001) 1108–1113.
[6] K. Teramura, T. Tanaka, H. Ishikawa, Y. Kohno, T. Funabiki, J. Phys. Chem. B 108 (2004) 346–354.
[7] K. Teramura, S. -i. Okuoka, H. Tsuneoka, T. Shishido, T. Tanaka, Appl. Catal. B: Environ. 96 (2010) 565–568.
[8] H. Tsuneoka, K. Teramura, T. Shishido, T. Tanaka, J. Phys. Chem. C 114 (2010) 8892–8898.
[9] F. Cavani, F. Trifirò, A. Vaccari, Catal. Today 11 (1991) 173–301.
[10] B.F. Sels, D.E. De Vos, P.A. Jacobs, Catal. Rev. 43 (2001) 443–488.
[11] C. Delhoyo, Appl. Clay Sci. 36 (2007) 103–121.
[12] K. Ebitani, K. Motokura, K. Mori, T. Mizugaki, K. Kaneda, J. Org. Chem. 71 (2006) 5440–5447.
[13] G. Abellan, E. Coronado, C. Marti-Gastaldo, J. Waerenborgh, A. Ribera, Inorg. Chem. 52 (2013) 10147–10157.
[14] F. Giovannelli, M. Zaghrioui, C. Autret-Lambert, F. Delorme, A. Seron, T. Chartier, B. Pignon, Mater. Chem. Phys. 137 (2012) 55–60.
[15] M. Gong, Y. Li, H. Wang, Y. Liang, J.Z. Wu, J. Zhou, J. Wang, T. Regier, F. Wei, H. Dai, J. Am. Chem. Soc. 135 (2013) 8452–8455.
[16] Y. Guo, Z. Zhu, Y. Qiu, J. Zhao, J. Hazard. Mater. 239–240 (2012) 279–288.
[17] L. Huang, S. Chu, J. Wang, F. Kong, L. Luo, Y. Wang, Z. Zou, Catal. Today 212 (2013) 81–88.
[18] T. Iwasaki, H. Yoshii, H. Nakamura, S. Watano, Appl. Clay Sci. 58 (2012) 120–124.
[19] B. Li, Y. Zhao, S. Zhang, W. Gao, M. Wei, ACS Appl. Mater. Interfaces 5 (2013) 10233–10239.
[20] H. Lin, Y. Zhang, G. Wang, J.-B. Li, Front. Mater. Sci. 6 (2012) 142–148.
[21] J. Prince, F. Tzompantzi, G. Mendoza-Damián, F. Hernández-Beltrán, J.S. Valente, Appl. Catal. B: Environ. 163 (2015) 352–360.
[22] F.B. Saiah, B.L. Su, N. Bettahar, J. Hazard. Mater. 165 (2009) 206–217.
[23] C.G. Silva, Y. Bouizi, V. Fornés, H. García, J. Am. Chem. Soc. 131 (2009) 13833–13839.
[24] F. Song, X. Hu, J. Am. Chem. Soc. 136 (2014) 16481–16484.
[25] T. Takei, A. Miura, N. Kumada, K. Okada, J. Porous Mater. 20 (2012) 777–783.
[26] L. Tian, Y. Zhao, S. He, M. Wei, X. Duan, Chem. Eng. J. 184 (2012) 261–267.
[27] X. Xu, R. Lu, X. Zhao, S. Xu, X. Lei, F. Zhang, D.G. Evans, Appl. Catal. B: Environ. 102 (2011) 147–156.
[28] X. Zhang, Z. Wang, N. Qiao, S. Qu, Z. Hao, ACS Catal. 4 (2014) 1500–1510.
[29] L. Mohapatra, K.M. Parida, Sep. Purif. Technol. 91 (2012) 73–80.
[30] L. Mohapatra, K.M. Parida, Phys. Chem. Chem. Phys. 16 (2014) 16985–16996.
[31] M. Shao, J. Han, M. Wei, D.G. Evans, X. Duan, Chem. Eng. J. 168 (2011) 519–524.
[32] J. Sun, Y. Zhang, J. Cheng, H. Fan, J. Zhu, X. Wang, S. Ai, J. Mol. Catal. A: Chem. 382 (2014) 146–153.
[33] S.J. Xia, F.X. Liu, Z.M. Ni, J.L. Xue, P.P. Qian, J. Colloid Interface Sci. 405 (2013) 195–200.
[34] J. Hong, Y. Wang, J. Pan, Z. Zhong, R. Xu, Nanoscale 3 (2011) 4655–4661.
[35] Y. Zhao, P. Chen, B. Zhang, D.S. Su, S. Zhang, L. Tian, J. Lu, Z. Li, X. Cao, B. Wang, M. Wei, D.G. Evans, X. Duan, Chemistry 18 (2012) 11949–11958.
[36] K. Teramura, S. Iguchi, Y. Mizuno, T. Shishido, T. Tanaka, Angew. Chem. Int. Ed. Engl. 51 (2012) 8008–8011.
[37] S. Iguchi, K. Teramura, S. Hosokawa, T. Tanaka, Catal. Today 251 (2015) 140–144.
[38] S. Iguchi, K. Teramura, S. Hosokawa, T. Tanaka, Phys. Chem. Chem. Phys. 17 (2015) 17995–18003.
[39] T. Mitsudome, Y. Mikami, H. Funai, T. Mizugaki, K. Jitsukawa, K. Kaneda, Angew. Chem. Int. Ed. 47 (2008) 138–141.
[40] T. Mitsudome, A. Noujima, T. Mizugaki, K. Jitsukawa, K. Kaneda, Adv. Synth. Catal. 351 (2009) 1890–1896.
[41] C. Pendem, P. Gupta, N. Chaudhary, S. Singh, J. Kumar, T. Sasaki, A. Datta, R. Bal, Green Chem. 14 (2012) 3107–3113.
[42] E.A. Gardner, S.K. Yun, T. Kwon, T.J. Pinnavaia, Appl. Clay Sci. 13 (1998) 479–494.
[43] D. Carriazo, S. Lima, C. Martín, M. Pillinger, A.A. Valente, V. Rives, J. Phys. Chem. Solids 68 (2007) 1872–1880.
[44] S. Omwoma, W. Chen, R. Tsunashima, Y.-F. Song, Coord. Chem. Rev. 258–259 (2014) 58–71.
[45] A. Corma, V. Fornes, F. Rey, A. Cervilla, E. Llopis, A. Ribera, Catal. Air J. Catal. 152 (1995) 237–242.
[46] M. Elena Pérez-Bernal, R. Ruano-Casero, T. Pinnavaia, Catal. Lett. 11 (1991) 55–61.
[47] E.P. Giannelis, D.G. Nocera, T.J. Pinnavaia, Inorg. Chem. 26 (1987) 203–205.
[48] U. Costantino, N. Coletti, M. Nocchetti, G.G. Aloisi, F. Elisei, Langmuir 15 (1999) 4454–4460.
[49] S. Pausova, J. Krysa, J. Jirkovsky, G. Mailhot, V. Prevot, Environ. Sci. Pollut. Res. Int. 19 (2012) 3709–3718.
[50] Z. Huang, P. Wu, Y. Lu, X. Wang, N. Zhu, Z. Dang, J. Hazard. Mater. 246–247 (2013) 70–78.
[51] J.S. Valente, F. Tzompantzi, J. Prince, Appl. Catal. B: Environ. 102 (2011) 276–285.
[52] E. Lima, M.d.J. Martínez-Ortiz, R.I.G. Reyes, M. Vera, Inorg. Chem. 51 (2012) 7774–7781.
[53] G. Wu, X. Wang, B. Chen, J. Li, N. Zhao, W. Wei, Y. Sun, Appl. Catal. A: Gen. 329 (2007) 106–111.
[54] G. Wu, X. Wang, W. Wei, Y. Sun, Appl. Cata. A: Gen. 377 (2010) 107–113.
[55] M.G. Álvarez, R.J. Chimentão, F. Figueras, F. Medina, Appl. Clay Sci. 58 (2012) 16–24.
[56] L. Moberg, B. Karlberg, Anal. Chim. Acta 407 (2000) 127–133.
[57] K. Carlsson, L. Moberg, B. Karlberg, Water Res. 33 (1999) 375–380.
[58] H.D.B. Jenkins, K.P. Thakur, J. Chem. Educ. 56 (1979) 576.
[59] N. Ahmed, Y. Shibata, T. Taniguchi, Y. Izumi, J. Catal. 279 (2011) 123–135.
[60] M. Morikawa, N. Ahmed, Y. Yoshida, Y. Izumi, Appl. Catal. B: Environ. 144 (2014) 561–569.
[61] M. Morikawa, Y. Ogura, N. Ahmed, S. Kawamura, G. Mikami, S. Okamoto, Y. Izumi, Catal. Sci. Technol. 4 (2014) 1644–1651.
[62] K. Katsumata, K. Sakai, K. Ikeda, G. Carja, N. Matsushita, K. Okada, Mater. Lett. 107 (2013) 138–140.

Please cite this article in press as: S. Iguchi, et al., Appl. Catal. A: Gen. (2015), http://dx.doi.org/10.1016/j.apcata.2015.11.023